ISSN 0915-633X

NATIONAL INSTITUTE FOR FUSION SCIENCE

Magnetization of a Two-Dimensional Electron Gas with a Spin-orbit Interaction

N. Hatano, R. Shirasaki and H. Nakamura

(Received - Mar. 13, 2006)

NIFS-832 Apr. 2006

RESEARCH REPORT
NIFS Series

TOKI, JAPAN

Magnetization of a two-dimensional electron gas with a spin-orbit interaction

Naomichi HATANO[1]*, Ryōen SHIRASAKI[2]†, and Hiroaki NAKAMURA[3]‡

[1] *Institute of Industrial Science, University of Tokyo, Komaba, Meguro, Tokyo 153-8505*
[2] *Department of Physics, Yokohama National University, Tokiwadai, Hodogaya-ku, Yokohama, Kanagawa 240-8501*
[3] *Theory and Computer Simulation Center, National Institute for Fusion Science, Oroshi-cho, Toki, Gifu 509-5292*

We argue that a two-dimensional electron gas with a spin-orbit interaction is magnetized when a voltage is applied with the Fermi level tuned to be in the energy gap. The magnetization is an indication of spin-carrying currents due to the spin-orbit interaction.

KEYWORDS: Rashba spin-orbit interaction, Dresselhaus spin-orbit interaction, two-dimensional electron gas, spintronics

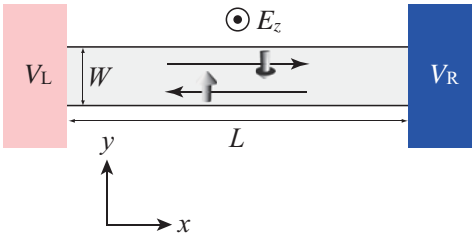

Fig. 1. A quantum wire under a voltage gradient.

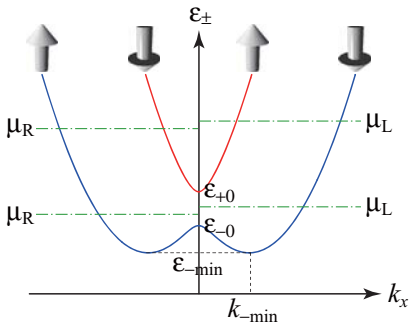

Fig. 2. A schematic view of the dispersion relations of the upper and lower bands of a channel. The right-going current has a chemical potential $\mu_L = -|e|V_L$ of the left contact, while the left-going current has a chemical potential $\mu_R = -|e|V_R$ of the right contact.

In the present article, we consider a two-dimensional electron gas with the Rashba or Dresselhaus spin-orbit interaction.[1–4] We argue that the system is magnetized when a voltage is applied (Fig. 1) with the chemical potential tuned to be in the energy gap. The magnetization indicates spin-carrying currents due to the spin-orbit interaction.

The spin current due to spin-orbit interactions is of great interest recently, particularly from the viewpoint of spintronics;[5–7] we could control the dynamics of spins with an external electric field. The spin current is predicted theoretically but has not been confirmed experimentally. How can we detect a spin current? We propose experimental observation of the magnetization that we predict here. The magnetization will imply underlying spin currents.

The following mechanism yields the magnetization. A spin-orbit interaction in the Hamiltonian has two effects on the dispersion of a channel (Fig. 2): first, the dispersion of up-spin electrons and the dispersion of down-spin electrons, respectively, shift sideways in the opposite directions; next, the crossing of the dispersions at $k_x = 0$ opens up an energy gap. Under this dispersion, we consider a simple theoretical state called the non-equilibrium steady state;[8–10] the right-going current has the Fermi distribution of the left contact while the left-going current has the Fermi distribution of the right contact and they run ballistically and independently. When the chemical potentials (the Fermi levels) of the right and left contacts are tuned to be in the energy gap of the dispersion, the number of up-spin electrons in the left-going current and the number of down-spin electrons in the right-going current can differ, and thereby appears the magnetization. This argument does not apply when the chemical potential is in the middle of a band, where the right-going up-spin electrons cancel the magnetization of the right-going down-spin electrons.

Let us begin the explanation with the Rashba system. The treatment of the Dresselhaus system is not much different. The Hamiltonian of the system with the Rashba spin-orbit interaction is given by[11]

$$\hat{\mathcal{H}} = \frac{1}{2m^*}\left(\hat{p}_x^2 + \hat{p}_y^2\right) + \alpha_{\rm RSO}\left(\hat{p}_x\hat{\sigma}_y - \hat{p}_y\hat{\sigma}_x\right), \qquad (1)$$

where m^* denotes the effective mass of an electron and $\alpha_{\rm RSO}$ denotes the strength of the Rashba interaction. We choose the y direction as the quantization axis of the electron spin and hence use the following representations hereafter:

$$\hat{\sigma}_x = \begin{pmatrix} 0 & 1 \\ 1 & 0 \end{pmatrix}, \qquad (2)$$

$$\hat{\sigma}_y = \begin{pmatrix} 1 & 0 \\ 0 & -1 \end{pmatrix}, \qquad (3)$$

$$\hat{\sigma}_z = \begin{pmatrix} 0 & i \\ -i & 0 \end{pmatrix}. \qquad (4)$$

*E-mail address: hatano@iis.u-tokyo.ac.jp
†E-mail address: sirasaki@phys.ynu.ac.jp
‡E-mail address: nakamura@tcsc.nifs.ac.jp

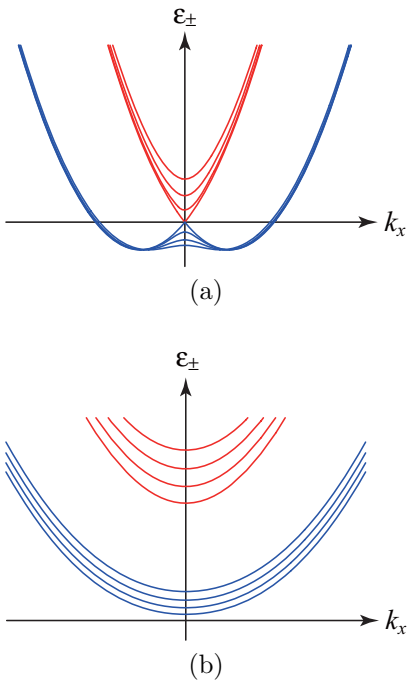

Fig. 3. A schematic view of the dispersion relation (8) for (a) some of the lowest channels and for (b) higher channels. The lowest channel has a real crossing at $k_x = 0$, but a higher channel has an avoided crossing. In (b), the double minima of the lower branch vanish for a high channel and the whole dispersion shifts upwards as we go to even higher channels.

The system is of length L in the x direction and of width W in the y direction with $W \ll L \ll$ mean free path. Hence the electrons run along the quantum wire ballistically through a few channels.

We first diagonalize the Hamiltonian (1) in the momentum space with the bases

$$|k_x, k_y, \sigma_y\rangle = \frac{1}{\sqrt{LW}} e^{i(k_x x + k_y y)} |\sigma_y\rangle , \tag{5}$$

where $k_y = 0, 2\pi/W, 4\pi/W, \ldots$ and $\sigma_y = \uparrow, \downarrow$.[12] The Hamiltonian (1) is given by a two-by-two matrix in the spin space in the form

$$\hat{\mathcal{H}} = \frac{\hbar^2}{2m^*} \left[k^2 + k\left(\hat{\sigma}_y \cos\phi - \hat{\sigma}_x \sin\phi\right)\right], \tag{6}$$

where $k^2 \equiv {k_x}^2 + {k_y}^2$, $(k_x, k_y) = k(\cos\phi, \sin\phi)$ and $\theta \equiv 2m^*\alpha_{\rm RSO}/\hbar$. The spin rotation $\exp(i\phi\hat{\sigma}_z/2)$ gives the representation

$$\hat{\mathcal{H}} = \frac{\hbar^2}{2m^*} \left(k^2 + k\hat{\sigma}_y\right) \tag{7}$$

with the eigenvalues[13,14]

$$\varepsilon_\pm(k_x, k_y) = \frac{\hbar^2}{2m^*} \left(k^2 \pm \theta k\right), \tag{8}$$

where the positive sign denotes the upper band and the negative sign denotes the lower band. For the lowest channel $k_y = 0$, the dispersion has two branches of parabolas with up and down spins, respectively. In the higher channels $k_y > 0$, the two branches are mixed around the avoided crossing at $k_x = 0$ (Fig. 3(a)). Note that, away from the avoided crossing, the lower branch in the region $k_x \gg 0$ still predominantly has down spins while it almost has up spins in the region $k_x \ll 0$.

Incidentally, lower channels are nearly degenerate in the present system as is shown in Fig. 3(a). This near degeneracy may be lifted if we include a potential $U(y)$ in the Hamiltonian. As another remark, the double minima of the lower branch shown in Fig. 3(a) vanish in higher channels and their dispersion shifts upwards as we go to even higher channels (Fig. 3(b)). The algebra hereafter slightly changes in the latter case but the final result (18) below is still valid.

The density of states $D_\pm$ of each band of each channel is given by

$$\frac{1}{D_\pm} = \frac{2\pi}{L} \left|\frac{\partial\varepsilon_\pm}{\partial k_x}\right| = \frac{\pi\hbar^2}{m^* L} \frac{|k_x|}{k} \sqrt{\theta^2 + \frac{8m^*}{\hbar^2}\varepsilon_\pm}. \tag{9}$$

The group velocity in the x direction is

$$v_\pm = \frac{1}{\hbar}\frac{\partial}{\partial k_x}\varepsilon(k_x, k_y), \tag{10}$$

which is positive wherever the slope of the dispersion is positive. The spin rotation $\exp(i\phi\hat{\sigma}_z/2)$ changes the spin operator $\hat{\sigma}_y$ to $\hat{\sigma}_y\cos\phi + \hat{\sigma}_x\sin\phi$ and hence the magnetization per unit area in the y direction is

$$m_\pm = \pm\frac{\mu_B}{LW}\cos\phi = \pm\frac{\mu_B}{LW}\frac{k_x}{k}. \tag{11}$$

The right-going current originated in the left contact with the chemical potential $\mu_{\rm L}$ contains all the states with positive group velocities. Thus we have the magnetization per unit area of the right-going current in the form

$$\begin{aligned} m_{\rm R}(k_y) &= \left(\int_{-k_{-\min}}^{0} + \int_{k_{-\min}}^{\infty}\right) m_- f(\varepsilon_-; T, \mu_{\rm L}) \frac{dk_x}{2\pi/L} \\ &\quad + \int_0^\infty m_+ f(\varepsilon_+; T, \mu_{\rm L}) \frac{dk_x}{2\pi/L} \\ &= \frac{\mu_{\rm B} m^*}{\pi\hbar^2 W} \left(\int_{\varepsilon_{-\min}}^{\varepsilon_{-0}} - \int_{\varepsilon_{-\min}}^{\infty} + \int_{\varepsilon_{+0}}^{\infty}\right) \frac{f(\varepsilon; T, \mu_{\rm L})}{\sqrt{\theta^2 + \frac{8m^*}{\hbar^2}\varepsilon}} d\varepsilon \end{aligned} \tag{12}$$

for a channel, where $f(\varepsilon; T, \mu)$ denotes the Fermi distribution function with the temperature T and the chemical potential μ. We here defined for each channel the following variables:

$$k_{-\min}(k_y) \equiv \sqrt{\frac{\theta^2}{4} - {k_y}^2} \tag{13}$$

$$\varepsilon_{-\min} \equiv -\frac{\hbar^2\theta^2}{8m^*} \tag{14}$$

$$\varepsilon_{\pm 0}(k_y) \equiv \frac{\hbar^2}{2m^*}({k_y}^2 \pm \theta k_y); \tag{15}$$

see Fig. 2. We used Eq. (9) in changing the integration variable from k_x to ε in Eq. (12). We can likewise obtain the magnetization of the left-going current in the form

$$m_{\rm L}(k_y) = \frac{\mu_{\rm B} m^*}{\pi\hbar^2 W} \left(-\int_{\varepsilon_{-\min}}^{\varepsilon_{-0}} + \int_{\varepsilon_{-\min}}^{\infty} - \int_{\varepsilon_{+0}}^{\infty}\right)$$

$$\times \frac{f(\varepsilon;T,\mu_{\rm R})}{\sqrt{\theta^2+\frac{8m^*}{\hbar^2}\varepsilon}}d\varepsilon \tag{16}$$

The total magnetization per unit area is given by

$$M_{\rm tot} \equiv \sum_{k_y} M(k_y) \tag{17}$$

with

$$M(k_y) \equiv m_{\rm R}(k_y) + m_{\rm L}(k_y)$$

$$= -\frac{\mu_{\rm B}}{2\pi\hbar W}\int_{\varepsilon_{-0}(k_y)}^{\varepsilon_{+0}(k_y)} \frac{f(\varepsilon;T,\mu_{\rm L}) - f(\varepsilon;T,\mu_{\rm R})}{\sqrt{{\alpha_{\rm RSO}}^2 + 2\varepsilon/m^*}}d\varepsilon. \tag{18}$$

Note here that only the integration over the energy gap survives. This is consistent with what we described in Fig. 2.

Let us analyze the linear response. We define the chemical-potential bias as

$$\mu_{\rm L} = \mu + \frac{\Delta\mu}{2}, \quad \mu_{\rm R} = \mu - \frac{\Delta\mu}{2} \tag{19}$$

with $\Delta V = V_{\rm L} - V_{\rm R} = -\Delta\mu/|e|$. The expansion of Eq. (18) with respect to $\Delta\mu$ is followed by

$$\frac{M_{\rm tot}}{\Delta V} \simeq \sum_{k_y} M^{(1)}(k_y) \equiv \frac{\mu_{\rm B}|e|}{2\pi\hbar W}\sum_{k_y} B(k_y), \tag{20}$$

where

$$B(k_y) \equiv \int_{x_{-0}(k_y)}^{x_{+0}(k_y)} \frac{g(x)}{\sqrt{{\alpha_{\rm RSO}}^2 + 2(k_{\rm B}Tx+\mu)/m^*}}dx \tag{21}$$

with $g(x) \equiv [2\cosh(x/2)]^{-2}$ and $x_{\pm 0}(k_y) \equiv (\varepsilon_{\pm 0}(k_y) - \mu)/k_{\rm B}T$.

Figure 4 shows the result of numerical calculation, where we used the values for an InGaAs/InAlAs heterojunction:[15] $\alpha_{\rm RSO}\hbar = 3\times10^{-11}$[eV m] and $m^* = 0.041m_e$. We also set $W = 1[\mu$m]. We find in Fig. 4(a) a peak of the magnetization around the energy gap of the dispersion relation. We observe for $\Delta V = 1$[mV] the magnetization of the order of 10^{-10}[J/T/m^2], which translates to 10^{-5}[G] if we assume that the thickness of the heterojunction is 10[nm].[15] Figure 4(b) shows the contribution of each channel, $M_n \equiv M^{(1)}(2n\pi/W)$, to the total magnetization $M_{\rm tot}$ at $T = 1$[K]. We note that each contribution is finite over the range of the energy gap of the respective channel, which is indicated by each bar. In the present case, some of the energy gaps overlap and hence a sharp peak in Fig. 4(a).

Finally, the Hamiltonian with the Dresselhaus interaction takes the form[11]

$$\hat{\mathcal{H}} = \frac{1}{2m^*}\left(\hat{p}_x^2 + \hat{p}_y^2\right) + \alpha_{\rm DSO}\left(\hat{p}_x\hat{\sigma}_x - \hat{p}_y\hat{\sigma}_y\right). \tag{22}$$

The rest of the formulation is the same as above with $\theta \equiv 2m^*\alpha_{\rm DSO}/\hbar$ and with the spin representations

$$\hat{\sigma}_x = \begin{pmatrix} 1 & 0 \\ 0 & -1 \end{pmatrix}, \tag{23}$$

$$\hat{\sigma}_y = \begin{pmatrix} 0 & -i \\ i & 0 \end{pmatrix}, \tag{24}$$

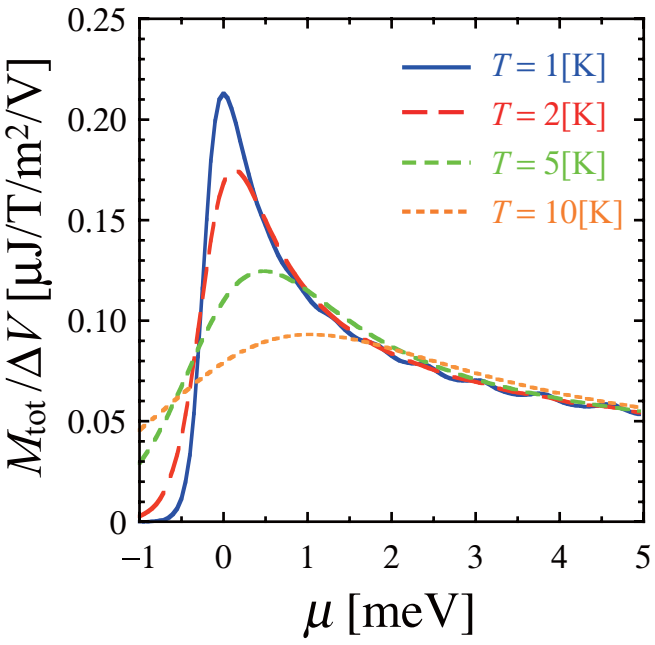

(a)

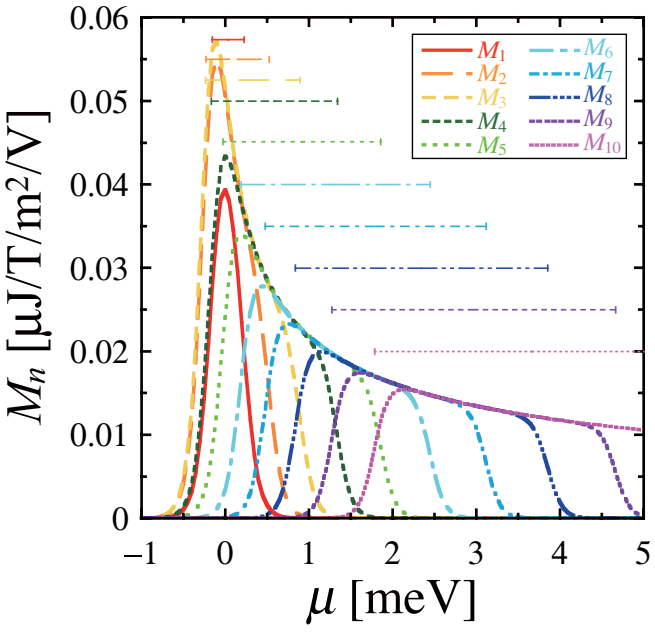

(b)

Fig. 4. (a) The response of the magnetization per unit area to the voltage bias ΔV. (b) Contributions $M_n \equiv M^{(1)}(2n\pi/W)$ from various channels for $T = 1$[K]. The bars indicate the energy gaps of the channels. In higher channels, the double minima at $k_x = k_{-\rm min}$ vanish and the "energy gap" shifts to the right.

$$\hat{\sigma}_z = \begin{pmatrix} 0 & -1 \\ -1 & 0 \end{pmatrix}. \tag{25}$$

The magnetization in the x direction is measured but the expression is the same as Eq. (18).

To summarize, we argued that the magnetization appears under a voltage gradient in systems with spin-orbit interactions when the Fermi levels are tuned to be in an energy gap. The magnetization is an indication of the spin-carrying current. Without taking account of any re-

laxation processes, the argument may be quite naive; we nevertheless believe that it is worth reporting and should be checked experimentally.

When we introduce a potential $U(y)$ into the Hamiltonians (1) and (22), the near degeneracy of the channels may be lifted. Then the magnetization should appear at the energy gap of every channel oscillatingly. We can also argue that the magnetization appears under a temperature gradient[16–18] rather than a voltage gradient; this effect will be reported elsewhere.

Acknowledgments

The work is supported partly by Grand-in Aid for Exploratory Research (No. 17654073) from the Ministry of Education, Culture, Sports, Science and Technology and partly by the Murata Science Foundation as well as by the National Institutes of Natural Sciences undertaking Forming Bases for Interdisciplinary and International Research through Cooperation Across Fields of Study. One of the authors (N.H.) acknowledges support by Grant-in-Aid for Scientific Research (No. 17340115) from the Ministry of Education, Culture, Sports, Science and Technology as well as support by Core Research for Evolutional Science and Technology of Japan Science and Technology Agency. The numerical integration in this work was done on a facility of the Supercomputer Center, Institute for Solid State Physics, University of Tokyo.

1) R.J. Elliott: Phys. Rev. **96** (1954) 266.
2) A. Messiah: "Quantum Mechanics" (Wiley & Sons, New York, 1958) Chap. XX, § 33.
3) E.I. Rashba: Fiz. Tverd. Tela (Leningrad) **2** (1960) 1224 [Sov. Phys. Solid State **2** (1960) 1109].
4) G. Dresselhaus: Phys. Rev. **100** (1955) 580.
5) I. Žutić, J. Fabian and S. Das Sarma: Rev. Mod. Phys. **76** (2004) 323.
6) S. Murakami, N. Nagaosa and S. Zhang: Science **301** (2003) 1348.
7) M. Eto, T. Hayashi and Y. Kurotani: J. Phys. Soc. Jpn. **74** (2005) 1934.
8) D. Ruelle: J. Stat. Phys. **98** (2000) 57.
9) Y. Ogata: Phys. Rev. E **66** (2002) 016135.
10) Y. Ogata: Phys. Rev. E **66** (2002) 066123.
11) E.I. Rashba: Phys. Rev. B **68** (2003) 241315(R).
12) For simplicity, we here imposed a periodic boundary condition in the y direction. Fixed boundaries would mix up various channels and make the solution much more complicated.
13) L.W. Molenkamp, G, Schmidt and G.E.W. Bauer: Phys. Rev. B **64** (2001) 121202(R).
14) P. Středa and P. Šeba: Phys. Rev. Lett. **90** (2003) 256601.
15) Y. Sato, T. Kita, S. Gozu and S. Yamada: J. Appl. Phys. **89** (2001) 8017.
16) H. Nakamura, N. Hatano and R. Shirasaki: Solid State Comm. **135** (2005) 510.
17) R. Shirasaki, H. Nakamura and N. Hatano: e-J. Surf. Sci. Nanotech. **3** (2005) 518.
18) H. Nakamura, N. Hatano and R. Shirasaki: to be published in "Proceedings of the 8th International Symposium on Foundations of Quantum Mechanics in the Light of New Technology - ISQM-Tokyo '05," eds. S. Ishioka and K. Fujikawa (World Scientific, Singapore); cond-mat/0509716.